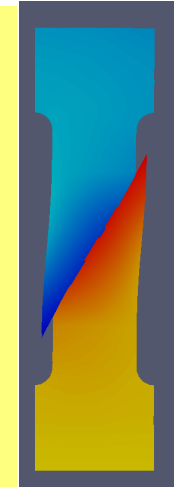
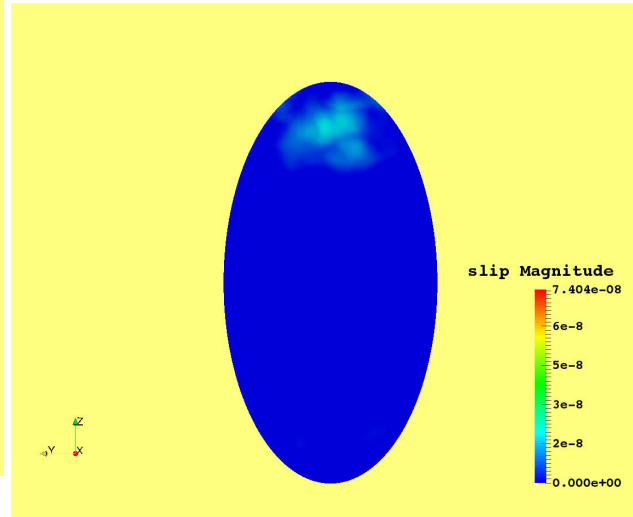
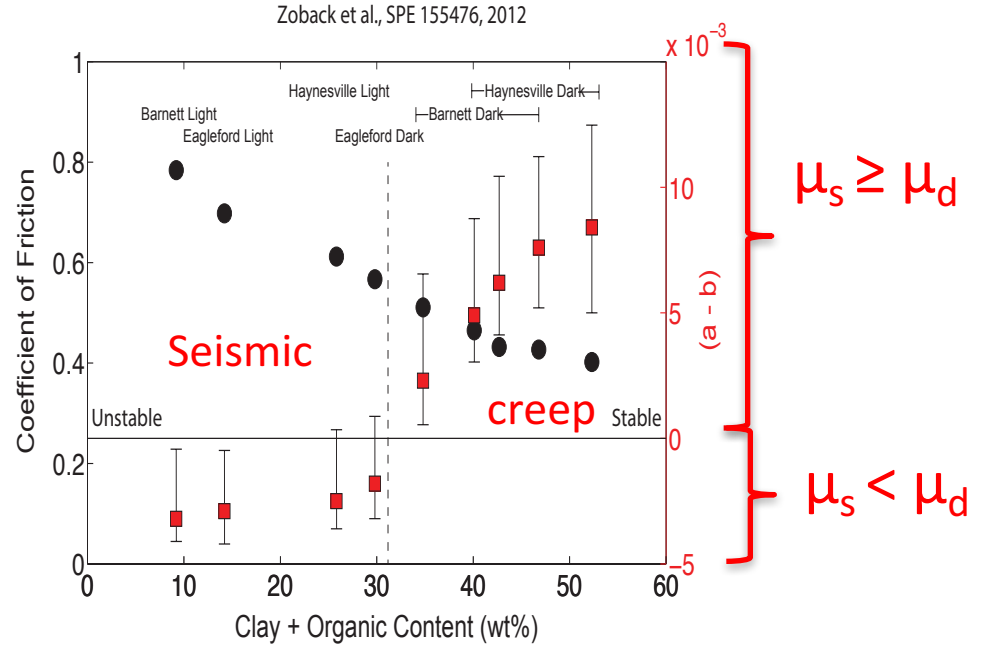
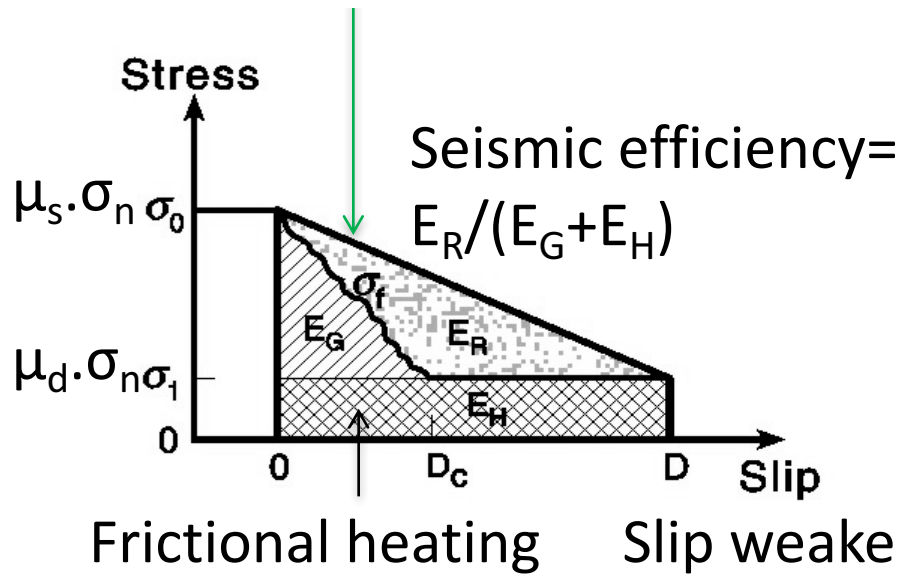


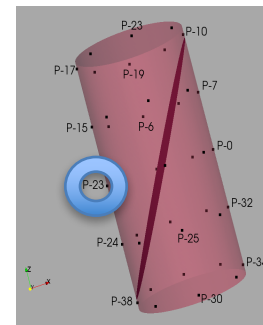
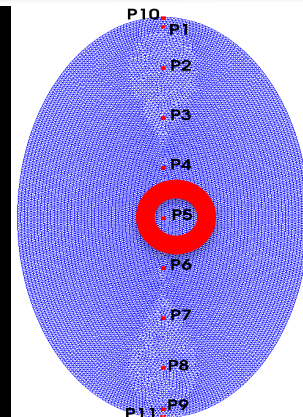
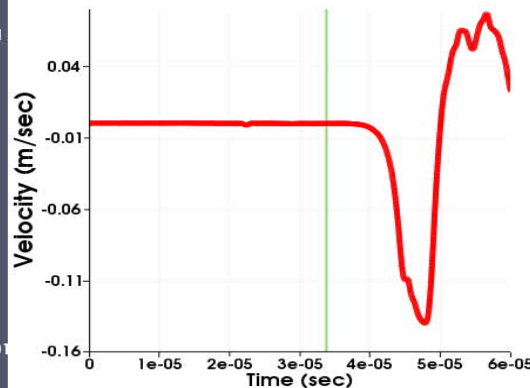
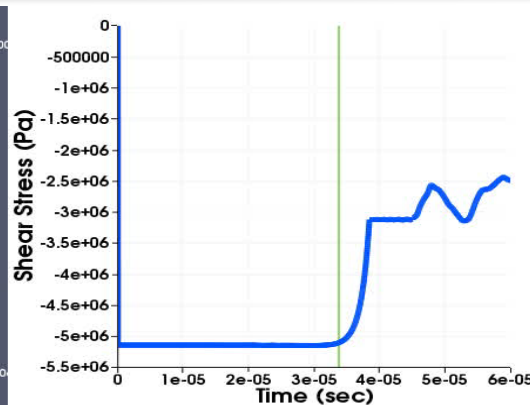
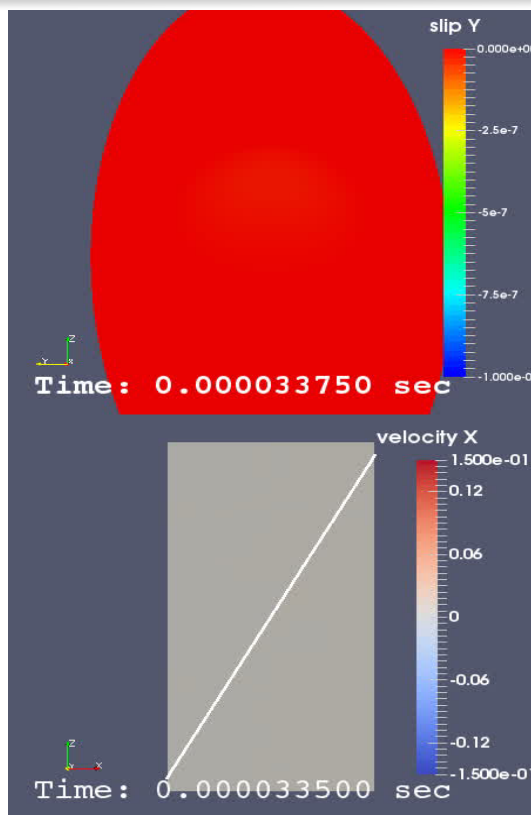
σ_{zz} on plane
perp to fracture



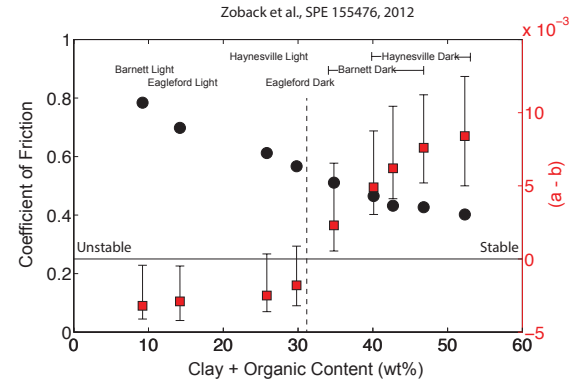
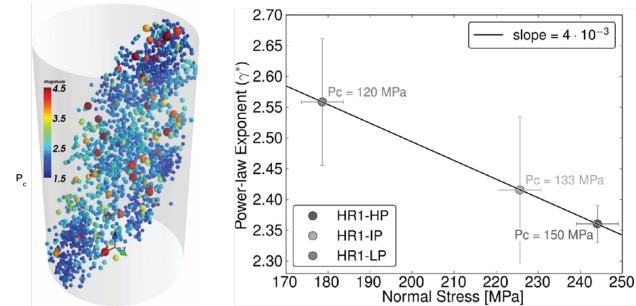
Displ. on plane
perp tp fracture

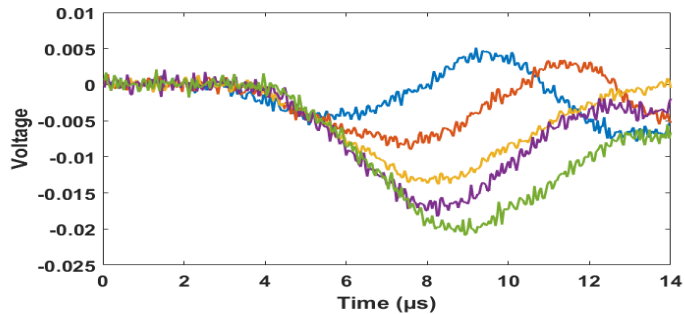
Slope depends on Elastic Modulus,
Fault Friction, and Fracture size



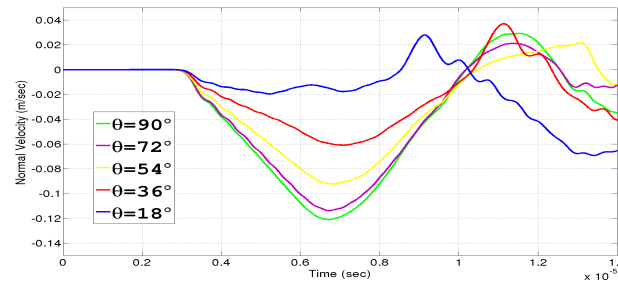


- Crystalline rocks at large d_{slip}
 - Roughness of secondary importance
 - Slip-weakening & rate-state friction
 - *Mature tectonic faults*
- Cryst. rocks w/ small d_{slip}
 - Width of AE locations
- k fault slip rate, G modulus, β power, H Hurst exponent ($H \uparrow$ roughness \uparrow)
- Width AE dist. \uparrow as Roughness & $\sigma_n \uparrow$
- Shale friction
 - Velocity weakening if clay+org >30%
 - Effects of roughness, normal load, effective pressure?

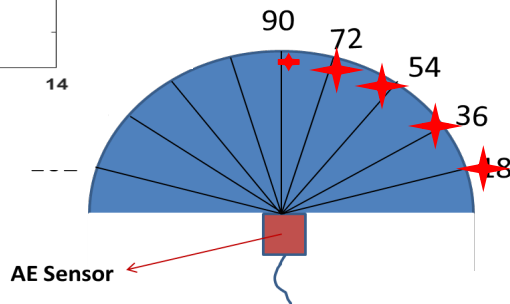




Measured Voltage



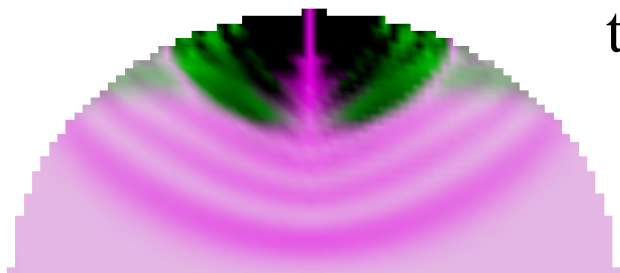
Calculated Velocity

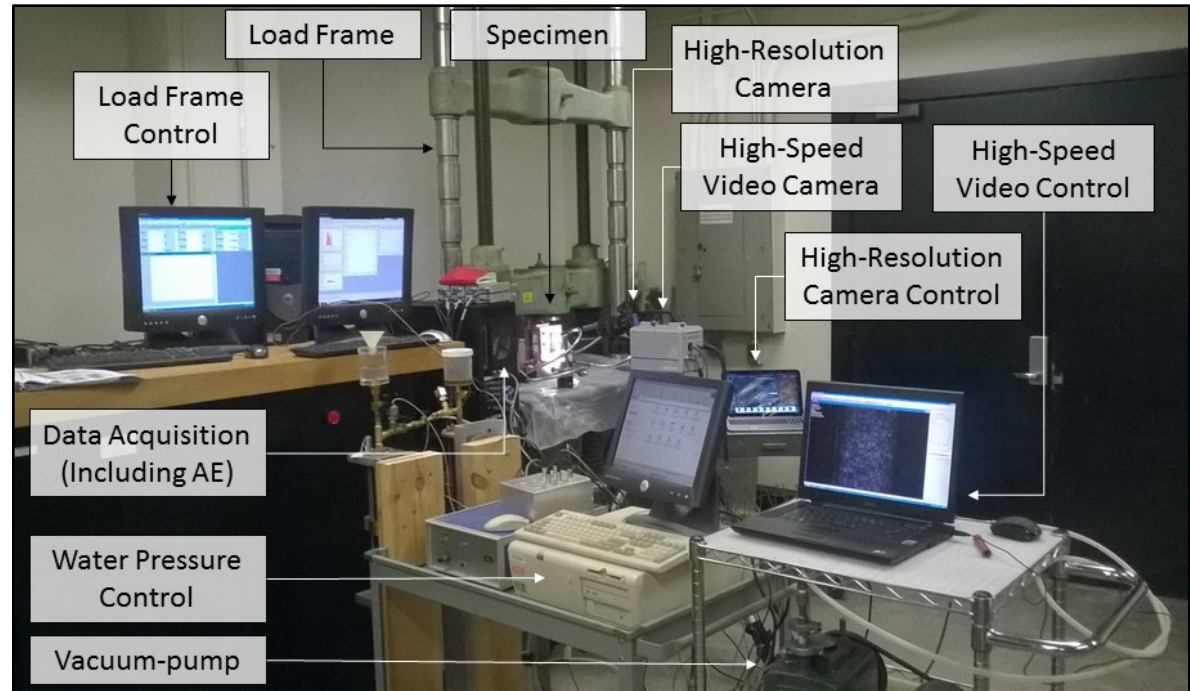
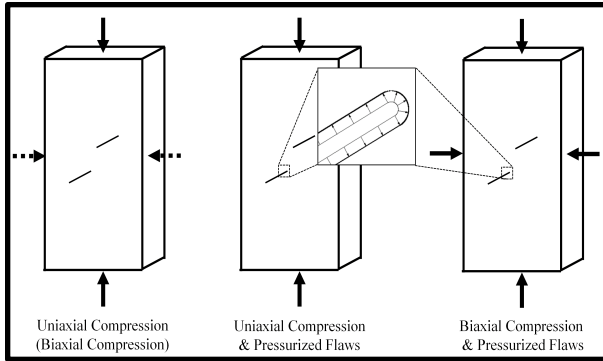


$t = 3.0 \mu\text{sec}$

18°

90°





Prismatic specimens, pre-existing flaws

Flaws can be internally pressurized

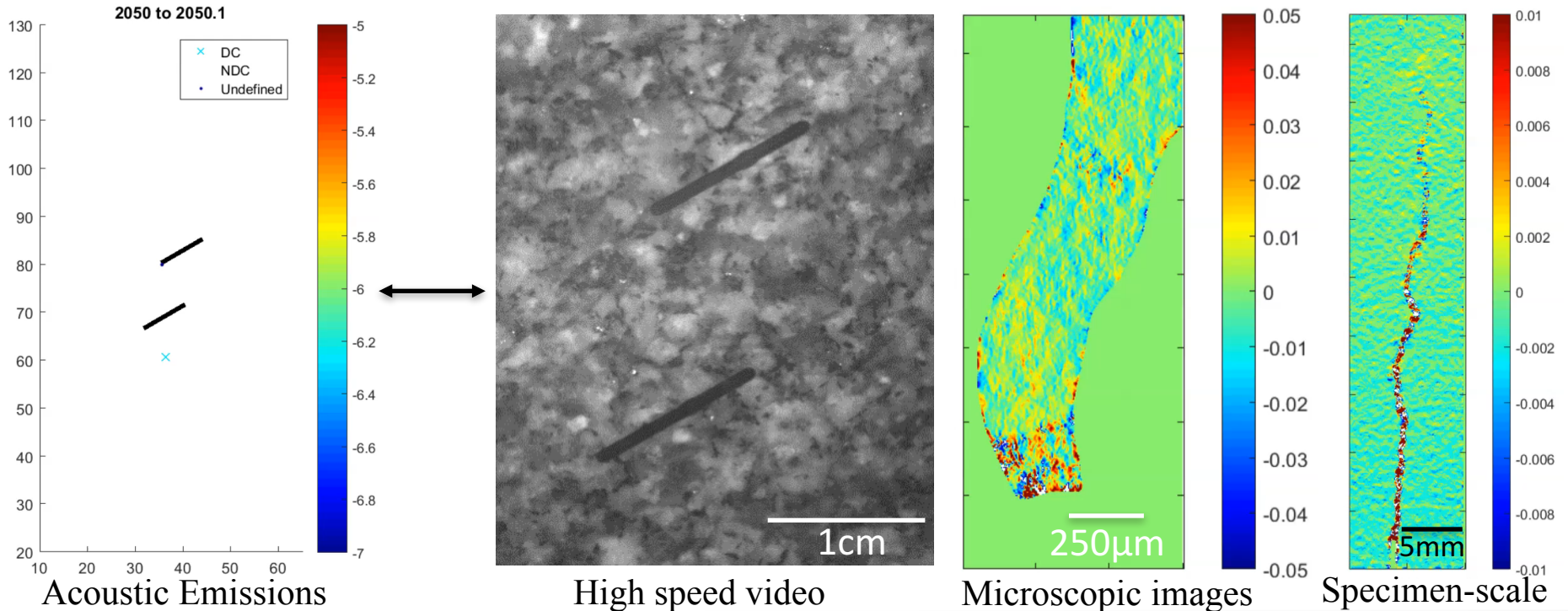
Uniaxial or biaxial external stresses

Visual (high speed and high resolution)

AE observations

Multiple observations of fracture initiation & propagation Slide 23

Bing Li: Relate visual observations to acoustic emissions (laboratory analogue to microseismicity), given that fractures are not directly accessible in the field.



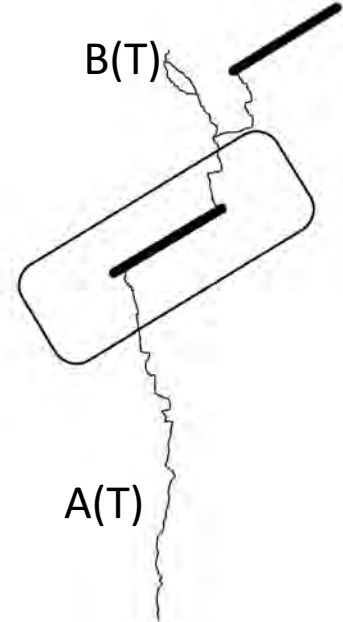
HF experiment showing crack tip ahead of fluid front



(Courtesy Omar Al Dajani)

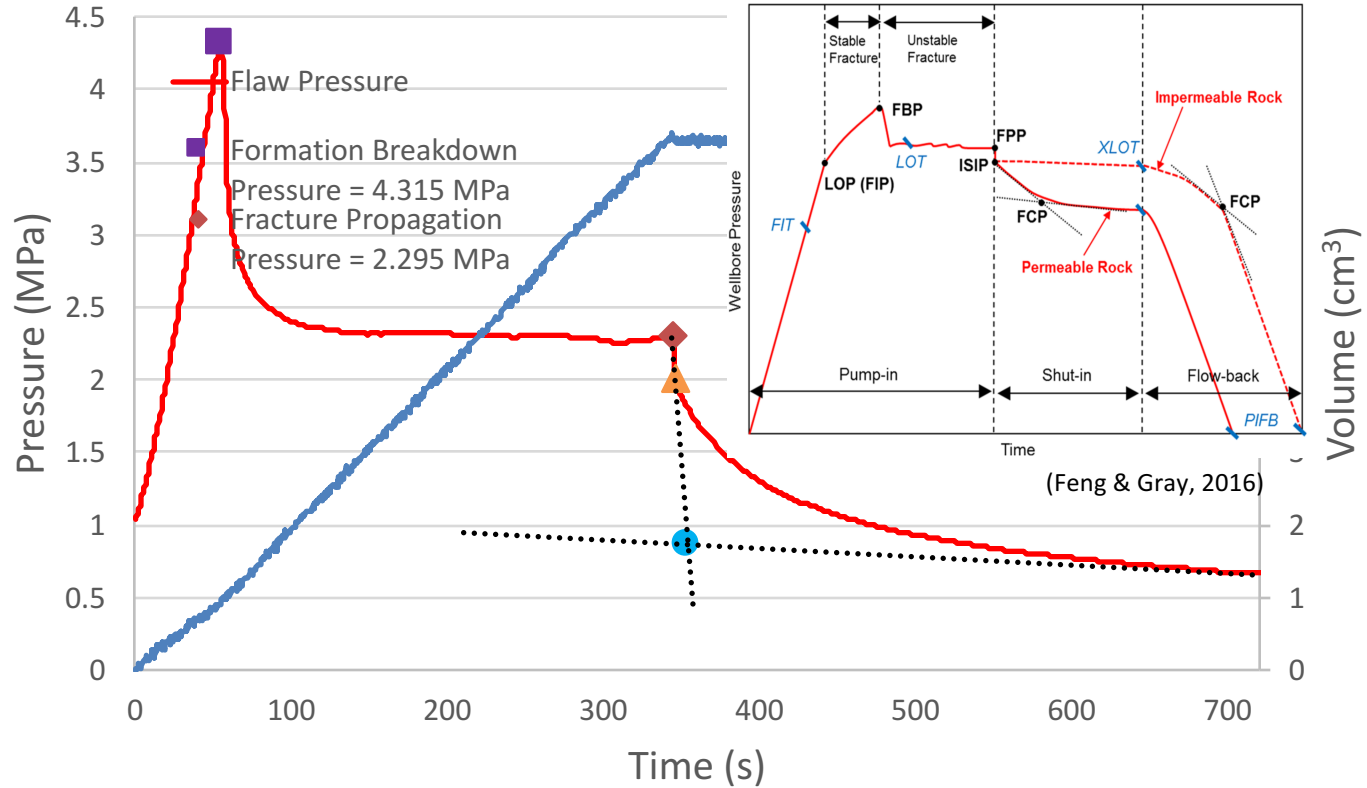


$$P_{\text{breakdown}} = 3.53 \text{ MPa}$$
$$V_{\text{injected}} = 2.461 \text{ cm}^3$$

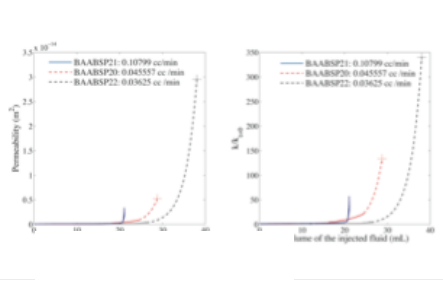


Equipment and results - low pressure HF experiments

HF experiment showing "classic" pressure time behavior



- Understanding processes associated with fractures is a rich problem.
- Combining Lab and Numerical investigations is a productive approach
 - Provide insights
 - Raise questions and paradoxes
 - Why are numerical earthquakes larger than AE events?
- ERL has special capabilities
 - High volume triaxial apparatus
 - Visualization of deformation via multiple approaches
 - Computation of quasi-static loading triggering dynamic failure, wave propagation
 - “realistic” fault failure parameterizations



Before dissolution

After breakthrough

- Core-flood in micritic, reef limestone
 - Flow rates >0.03 and <0.1 mL/min.
 - Pore fluid =H₂O sat. with CO₂, i.e., chemically reactive fluid
 - Rapid increases in k at "breakthrough"
- SEM and microtomography images
 - Wormhole develops in 3-18 hours with dramatically increasing permeability
- Numerical modeling
 - Pore-scale heterogeneity important
 - "Kinetic switch" along selected path
 - Spatial correlations greatly facilitate wormhole formation

Relations among mechanical behavior, fluid transmissivity and acoustic properties of joints (cont.)

- **Creep deformation: Effects of fluids**

- Pressure solution deformation
 $T \leq 600^\circ\text{C}$ $P_f \leq 200$ MPa
 micron scale pillars
- Cementation, fracturing
 and pressure solution
 - partitioning between mechanisms
 enigmatic

Work in progress, see also:

Fitzenz, D. D., Y. Bernabé, S. H. Hickman, and B. Evans (2008), Incorporating intergranular pressure solution into models of fault zone deformation, *EOS Trans. AGU*, 89(53), Fall Meet. Suppl., Abstract T53C-1965.

Bernabé, Y., B. Evans, and D. D. Fitzenz (2009), Stress transfer during pressure solution compression of rigidly coupled axisymmetric asperities pressed against a flat semi-infinite solid, *Pure and Applied Geophysics*, 166(5-7), 899-925, doi:10.1007/s00024-009-0477-2.

Bernabé, Y., and B. Evans (2014), Pressure solution creep of random packs of spheres, *Journal of Geophysical Research: Solid Earth*, 119(5), 4202-4218, doi:10.1002/2014jb011036

